On the possibility of implementing a simple shear in the cross-section of metal materials during caliber rolling

Maxat Abishkenov[a*], Zhassulan Ashkeyev[b], Kayrosh Nogaev[c], Yerbol Bestembek[b], Kuathan Azimbayev[a] and Ilgar Tavshanov[d]

[a]Master of Science, Department of Technological Machines and Transport, Karaganda Industrial University, 30 Republic Ave., 101400 Temirtau, Kazakhstan
[b]PhD, Associate Professor, Department of Technological Machines and Transport, Karaganda Industrial University, 30 Republic Ave., 101400 Temirtau, Kazakhstan
[c]PhD., Department of Technological Machines and Transport, Karaganda Industrial University, 30 Republic Ave., 101400 Temirtau, Kazakhstan
[d]Master's student, Department of Technological Machines and Transport, Karaganda Industrial University, 30 Republic Ave., 101400 Temirtau, Kazakhstan

A R T I C L E I N F O	A B S T R A C T
	The article analyzes the stress-strain state in the zone of plastic deformation during special caliber rolling. The principle of caliber rolling technology is described, which makes it possible to combine shear and compression deformations in the cross-section of metals, alloys, and metal-matrix composites. The analysis results of stresses and strains during shear rolling in a diamond pass, which included compressive strains that had not been considered in previous studies, revealed that localization or point inversion of stresses and strains is observed in the plastic deformation zone. Stress and strain are localized along the minor and major diagonals of the diamond pass.

1. Introduction

Rolling processes are widely used in modern metalworking because of their technological simplicity, productivity, continuity, and ability to produce metal materials in a variety of sizes and shapes. They are also of scientific interest in terms of developing new advanced rolling technologies. Technologies for creating shear strains in rolling processes are among the most appealing and promising of such developments. Methods or techniques for material processing based on shear deformations are very diverse regarding deformation modes. In the theory of deformations, simple shear and pure shear are distinguished, as in the first approximation, they differ from each other only in turn or rotation: simple shear, with rotation; pure shear, without rotation. These two concepts of the shift are still often confused in the literature. Researchers have proposed various approaches to explain their difference to avoid confusion, for example, in terms of the theory of Cauchy tensors (Thiel et al., 2018). Beygelzimer, the author of the twist extrusion development (Beygelzimer, 2009), reported in his research papers on simple shear. Simple shear is a two-stage process. At the first stage, in a certain range of shear deformation, the microstructure of the metal changes similarly to how it occurs in the process of elongation (pure shear). Then, at the second stage, when a certain critical shear stress is reached, the stationary, turbulent motions occur in the material. The second stage of deformation, in fact, is a simple shear. The physical reason for the existence of the second stage is the stress tensor asymmetry due to a connected network of high-angle boundaries that allow slippage and high pressure on the shear plane. Shear deformations determine both the macrocracks formation and the deformation effect on the original metal material. The main property of shear deformations is the reorientation of the crystal lattice due to atomic displacements or movement along

slope lines (Cao et al., 2018). This determines the flow macromechanism and is preserved for bodies with any rheological behavior.

Recently, the urgency of deformation modes developing that provide high-quality ultrafine-grained (UFG) or nanostructured (NS) metal materials (powder materials, pure metals and alloys, amorphous alloys, and metal-matrix composites) through high shear deformations has been growing. This fueled the development of special shear deformation techniques, such as severe plastic deformation (SPD) techniques, which today have become a generally accepted approach in material processing. Bridgman's pioneering experiments on the implementation of shear torsion with compression (this process was later called high-pressure torsion, HPT) under conditions of high hydrostatic pressures (usually several gigapascals) in solids (Bridgman, 1935) proved the possibility of obtaining unique properties in metallic materials and aroused further scientific and industrial interest in SPD techniques (Langdon, 2010; Bagherpour et al., 2019; Valiev et al., 2000; Cao et al., 2018).

In modern metallic materials engineering, the technological rolling and rotation principles are often used in a single technological cycle with other metalworking processes, such as SPD techniques. This is especially true for continuous equal channel angular extrusion/pressing (ECAE/ECAP) techniques, such as conshearing (Saito et al., 2000; Utsunomiya et al., 2004), continuous confined strip shearing (Lee et al., 2001; Peng et al., 2018), ECAP-Conform (Xu et al., 2010; Derakhshan et al., 2019), continuous frictional angular extrusion (Huang & Prangnell, 2007), integrated conventional tandem rolling with ECAP (Zhu et al., 2010), single-roll angular rolling (Lee et al., 2018), and equal channel angular rolling (Cheng et al., 2007; Song et al., 2018). In rolling processes, rolls are used to ensure continuity, but the shear deformation itself is carried out in ECA dies. Good properties and structure refinement of metallic materials are also observed in processes in which rolling is used separately, either before or after SPD, rather than in a single technological cycle with SPD techniques. Over the past decade, interest in such hybrid technologies has been growing permanently. This is primarily due to the high possibility of integrating such technologies into existing technological rolling chains without significant modifications. Examples of such hybrid technologies are rolling schemes with ECAP (Xu et al., 2021), HPT (Edalati et al., 2014), and multiaxial forging (Verma et al., 2020).

High productivity, industrialization opportunities, and technological ease of rolling have increased interest in developing rolling-based SPD techniques (Bagherpour et al., 2019). One technique that is successfully applied to the production of multilayer composite sheets is accumulative roll bonding (ARB) (Saito et al., 1999; Lee et al., 2002). The ARB process is very similar to conventional rolling; therefore, like conventional rolling, ARB produces elongated grain structures with typical rolling texture components, such as S {123}<634>, copper {112}<111>, and brass {011}<211> (Jamaati & Toroghinejad, 2014), regardless of the material type being processed. However, that does not mean that grain refinement in the ARB process occurs only due to the formation of a rolling texture with a large force and a number of deformation cycles. As in conventional rolling, during ARB, excessive shear deformation acts due to friction between the material being processed and the rolls along the thickness of the sheet in the plane of the normal direction (ND) to the rolling direction (RD) (Saito et al., 2000), which also affects the structure material refinement. However, in such a deformed state, the deformation gradient occurs along the thickness, leading to an inhomogeneous microstructure and texture, i.e., plastic anisotropy (Beausir et al., 2010). To obtain more isotropic materials, additional shear deformation can be introduced into the ARB process, which occurs, for example, when using asymmetric rolling (AR) (Camilo Magalhães et al., 2020) and, like ARB, is a rolling-based SPD technique (Cui & Ohori, 2000). With AR, different roll speeds, sizes, or configurations create opposing frictional forces at the top and bottom of the material, creating shear stresses throughout the material. Thus, compression deformation in the ND is complemented by shear deformation, which affects the transition from rolling texture to shear texture. This means that favorable conditions are created in the plastic deformation zone to prevent the structure from stretching and reduce dangerous tensile stresses, all of which contribute to the alignment of the values of mechanical property, internal defects elimination, and ultimately obtaining more isotropic materials (Ashkeyev et al., 2020). Another SPD technique based on rolling is repetitive corrugation and straightening via rolling (RCSR), in which shear deformation is realized and accumulated either in the longitudinal (Huang et al., 2001) or in the cross-section (Mirsepasi et al., 2012) of the material with minor dimensional changes. The process is promising for UFG/NS metal sheet production. And finally, it should be noted that the technological rolling simplicity has provided the preconditions for the developments in the field of rolling at ultralow cryogenic temperatures since structural and phase changes occur at such temperatures, which favorably affect the material properties. These processes are collectively known as cryorolling and are also applicable to traditional rolling (Zherebtsov et al., 2013; Li et al., 2021) and special rolling methods (Afifeh et al., 2019; Yu et al., 2019).

The analysis of the available sources revealed the most common techniques for shear deformations during sheet rolling; however, there are practically no such techniques for sectional (profile) rolling and the available ones are hybrid technologies, where shear does not act during rolling. Rolling is only used for pulling dimensional operations or radial shear rolling techniques (Mashekov et al., 2021), which have characteristic limitations in terms of product range and are technologically complex. Moreover, the literature analysis revealed that in the known shear rolling processes, the shear acts mainly in the longitudinal section of the material being processed and not in the transverse one. This study presents the analysis results of the stress-strain state of a material subjected to simple shear during caliber rolling. Simple shear during caliber rolling acts in the transverse section of the material.

2. The principle of caliber rolling technology with transverse simple shear

Previous studies on the simple shear upsetting (SSU) process (Naizabekov & Ashkeev, 1995, 1998; Naizabekov et al., 1999; Najzabekov et al., 2004; Ashkeyev et al., 2023) served as the forerunners for the development of the technology. According to these studies, the action of shear deformations in the internal zones can positively influence the structure of the metallic material and reduce the process force parameters. Forging, like rolling, is a metal-forming process with excellent potential for producing large-sized metal materials through shear deformation, and it is also technologically simple, making research in this area very relevant. This can be confirmed by a recent study of the new SPD technique (Rahimi Goloujeh & Soltanpour, 2021) with the application of hydrostatic pressure on the metal material and the ability not to change the cross-sectional area, which ensures the repeatability of the process. Based on the good results of the works by (Naizabekov & Ashkeev, 1995, 1998; Naizabekov et al., 1999; Najzabekov et al., 2004; Ashkeyev et al., 2023; Rahimi Goloujeh & Soltanpour, 2021), the concept of generating a simple shear in the transverse section of the material during sectional rolling and in the longitudinal section of the material during drawing was developed. This resulted in shear caliber rolling in a special diamond-square pass rolling sequence (Naizabekov et al., 2010; Abishkenov et al., 2022).

Fig. 1 shows a schematic representation of the rolling technology. Here, the rolling process is based on the fact that the usual (traditional) diamond-diamond passes are replaced with special diamond passes (1, 3, 5, 7), in which a transverse simple shear is implemented, while square passes (2, 4, 6, 7) remain unchanged; i.e., simple shear in diamond passes alternates with compression strains in square passes. In addition, reduction also acts in the diamond passes. The oval 9 and 10 round passes are the prefinish and finish passes, respectively. The shift angle γ in diamond passes is 40º. Roll pass design allows for alternating deformation in the cross-section of diamond passes; i.e., the simple shear direction in diamond passes 1 and 5 is opposite to the simple shear direction in diamond passes 3 and 7, respectively. This alternation of simple shear directions is similar to the shear alternation described in the study by Rahimi Goloujeh & Soltanpour (2021) with one difference: in the study by Rahimi Goloujeh & Soltanpour (2021), the return of the sample to its original shape after shear is carried out by material loading with another transverse shear strain. In our case, such a return to a square shape is carried out by loading the material with compressive deformation in square passes. As a result of the action of transverse simple shear, two plastic flows with opposite direction vectors arise in the plastic deformation zone (Abishkenov et al., 2022). The inclined portions of the upper and lower rolls generated the simple shear. Turning the samples in each subsequent pass (the angles of rotation are shown in Fig. 1) leads to the renewal of the corners of the material in direct contact with the walls of the rolls, which prevents local overcooling of individual sections of the material, thereby reducing the wear rate of the rolls. In terms of positioning or cutting on the rolls, special diamond passes are more similar to conventional box passes (grooves) than conventional diamond passes, which helps reduce the caliber cut depth, making the roll more stable and durable. If necessary, the entire rolling process can be carried out during several similar cycles, which depends on the requirements for the quality of metal materials, and the dimensions ratio of the initial workpiece and the final product.
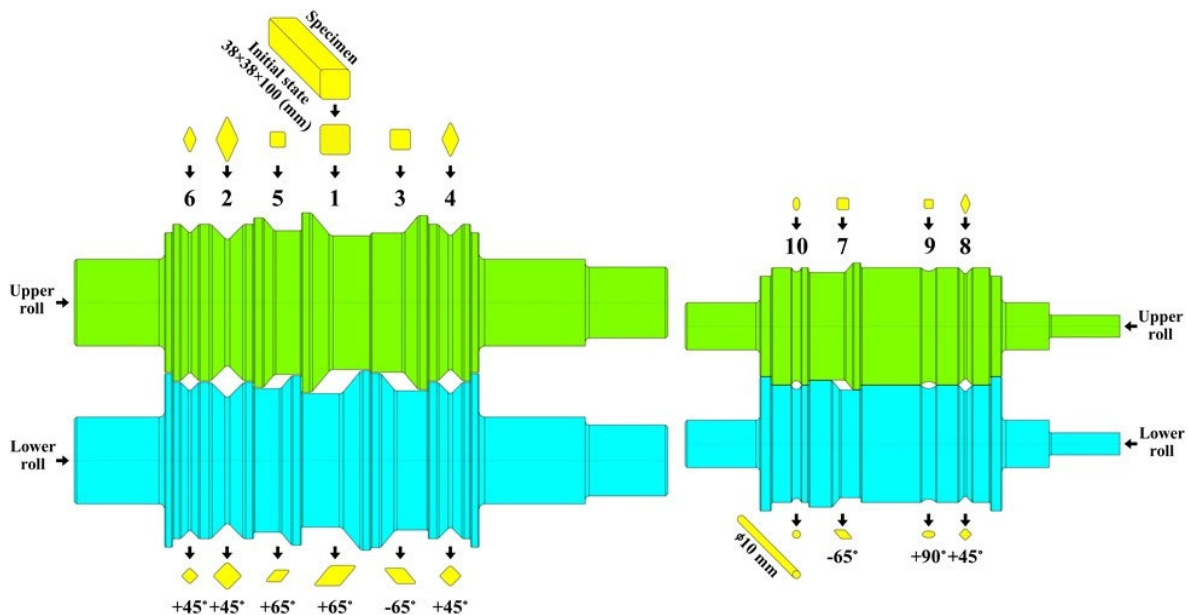

Fig. 1. Caliber rolling process with transverse simple shear: 1, 2, 3, … 10 are the rolling passes; +45°, ±65°, and +90° are the rotation angles of the metal sample before it enters the next pass.

3. Analysis of stresses and strains in the plastic deformation zone under simple shear in a diamond pass

The stress distribution analysis in the plastic deformation zone is the most important element in proving the effectiveness of using metal-forming technology to improve the structure of a ductile metal material and the quality of the resulting final product. In the present study, the classical slip line method was used for such an analysis. The slip lines field was compared with the stress pattern obtained by the finite element method (FEM) on the commercial FEM code DEFORM-3D. Previously, a preliminary analysis of the material stress state during shear rolling using the slide line method (Abishkenov et al., 2022) revealed that shear is indeed observed in the cross-section of the material. However, this simplified analysis of stresses in the plastic deformation zone was carried out only considering a simple shear in the cross-section of the rolled material. When rolling in diamond passes, in addition to shear deformation, the metal material is also subjected to compression deformations from the horizontal working surfaces of the roll passes (Fig. 1). Therefore, in the present study, an additional analysis was carried out taking into account the combined effect of shear and compression deformations. The analysis was carried out by the slip line method, which was previously successfully applied by the authors in the stress-strain state analysis of materials subjected to shear deformations (Ashkeyev et al., 2020, 2021a, 2021b, 2023; Abishkenov et al., 2022). The slip line method or the plane strain modeling approach of a rigid-plastic isotropic solid body under a quasistatic load without taking into account the elasticity and work hardening of this body and temperature parameters is currently largely superseded by the FEM, which can analyze temperature, structure, phase, and deformation parameters of existing and special plastic deformation techniques under complex loads. However, this method, based on plastic flow along slip lines, is a commonly used method for stress and force analysis, as it offers the simplest way to solve plane strain equilibrium equations by expressing stresses in terms of nodal points in a coordinate system (because stress can vary from point to point). For this, it is necessary to construct a slip lines field. The construction or drawing of the slip lines field begins with the contact surface (the length of which is equal to the length between points a and b in Fig. 2), where the slip lines are at an angle α, the value of which depends on the friction coefficient f (preliminarily taken equal to the average value ~ 0.25), by the following ratio:

$$f = \frac{\cos 2\alpha}{2}, \tag{1}$$

From Eq. (1), we can see that $\alpha = 30°$. From geometric considerations, it is easy to see that the inclination angle of the slip line to the y-axis at the nodal point 1.2 will be $\theta_{1.2} = 45°$. The angles of inclination at the other nodal points are determined by taking the step of changing the slip lines $\Delta\theta = 10°$. From this, it follows that the values of the slip lines' inclination angles $\theta_{0.1}$ and $\theta_{1.1}$, respectively, passing through the neighboring corner points 0.1 and 1.1, are determined from the following equations:

$$\theta_{0,1} = \theta_{1,2} + \Delta\theta, \tag{2a}$$

$$\theta_{1,1} = \theta_{1,2} - \Delta\theta. \tag{2b}$$

Eq. (2a) and Eq. (2b) yield $\theta_{0.1} = 55°$ and $\theta_{1.1} = 35°$. It follows from the fundamental principles of the theory of slip lines (Rees, 2006) that these slip lines passing through points 0.1 and 1.1 must intersect at an angle of 45° with the x- and y-axes at the central point 0.0:

$$\theta_{0,0} = \frac{\theta_{0,1} + \theta_{1,1}}{2} = 45°, \tag{3}$$

Substituting the angle values into Eq. (3), it can be verified that the slip lines intersect at an angle of 45° with the x- and y-symmetry axes. This indicates the correctness of the slip lines net construction since the main axes intersect with the maximum shear stresses τ_{max} exactly at an angle of 45°, as seen in Fig. 2(a). Moreover, the correctness of the slip lines field construction confirms the kinematic possible velocity field shown in Fig. 2(b), where from the condition of the deformable body incompressibility, we can write the following:

$$v_0 \times |ab| = v_1 \times h \;\rightarrow\; \frac{v_1}{v_0} = \frac{|ab|}{h} \sim 0{,}7 \div 0{,}72 \tag{4}$$

where |ab| is the strip contact zone length with the rolls' working surface, h is the sample current height, v_0 is the material points speed along the y-axis or the points speed in the direction of the sample height, and v_1 is the material points speed along the sample width. Next, the stress state is determined at the central axial nodal point 0.0 according to the constructed slip lines field in Fig. 2(a). From the equilibrium condition for the forces applied to the plastic region on the right, taking into account the signs relative to the y-axis, we can write the following:

$$\int_{0,0}^{0,1} \sigma dy + kx_{0,2} + \sigma_{0,1}\left(y_{0,2} - y_{0,1}\right) + \int_{0,1'}^{0,0} \sigma' dy + kx_{2,2'} + \sigma_{1,1'}\left(y_{1,1'} - y_{2,2'}\right) = 0 \tag{5}$$

where $y_{0.1}$, $y_{0.2}$, $y_{1.1'}$, $y_{2.2'}$, $x_{0.2}$, and $x_{2.2'}$ are the coordinates of the nodal points along the y- and x-axes at the respective nodal points indicated in subscripts, σ is the normal mean stress along the slip line 0.0–0.1, $\sigma_{0.1}$ is the average normal stress at the nodal point 0.1, σ' is the average normal stress along the slip lines 0.0–1.1', $\sigma_{1.1'}$ is the average normal stress at the nodal point 1.1', and k is plasticity constant or shear yield stress independent of x and y.

Using Hencky equations (Rees, 2006; Ashkeyev et al., 2020, 2021a, 2021b, 2023; Abishkenov et al., 2022), the expressions are derived to determine the mean normal stresses:

$$\sigma = \sigma_{0,0} - 2k\left(\theta - \frac{\pi}{4}\right), \tag{6.a}$$

$$\sigma_{0,1} = \sigma_{0,0} - 2k\left(\theta_{0,1} - \frac{\pi}{4}\right) \tag{6b}$$

$$\sigma' = \sigma_{0,0} + 2k\left(\theta' - \frac{\pi}{4}\right), \tag{6.c}$$

$$\sigma_{1,1'} = \sigma_{00} + 2k\left(\theta_{1,1'} - \frac{\pi}{4}\right), \tag{6.d}$$

where θ and θ', respectively, are the average values of the tangents inclination angles along the slip lines 0.0–0.1 and 0.0–1.1', $\theta_{0.1}$ and $\theta_{1.1'}$, respectively, are the angles between the tangent to the slip lines passing through the points 0.1 and 0.1' and the principal axes.
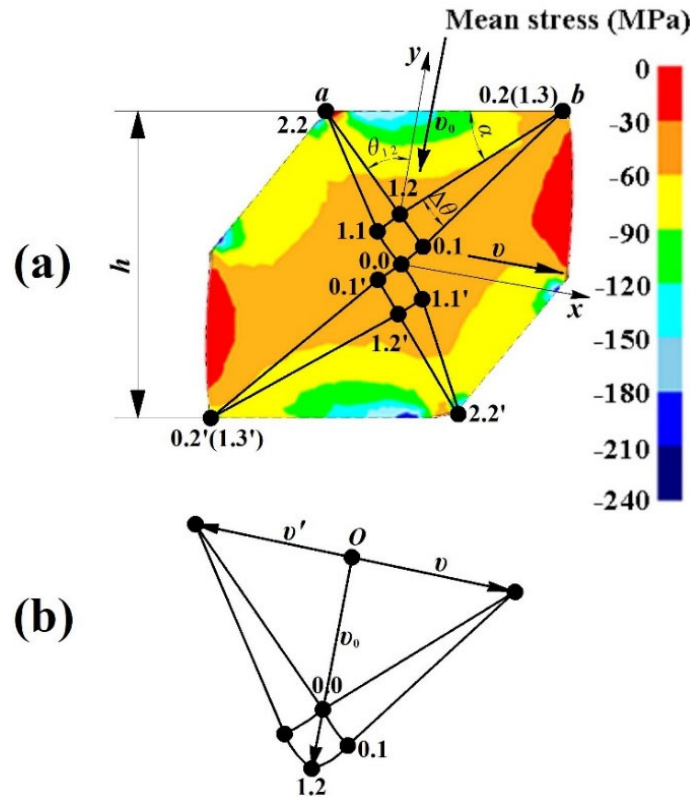

Fig. 2. The field of slip lines in the plastic deformation zone during shear rolling of a metal material in a diamond pass superimposed on the stress state image obtained by the finite element method (FEM) on the commercial FEM code DEFORM-3D (a) and the velocity hodograph (b).

Substituting Eqs. (6.a), (6.b), (6.c), (6.d) in Eq. (5) and solving the resulting equation with respect to $\sigma_{0.0}$, the result will be an equation that takes the following form:

$$\frac{\sigma_{0,0}}{2k} = \frac{\left(\theta - \frac{\pi}{4}\right)y_{0,1} + \left(\theta_{0,1} - \frac{\pi}{4}\right)\left(y_{0,2} - y_{0,1}\right) - 0,5\left(x_{0,2} + x_{2,2'}\right)}{\left(y_{0,2} - y_{2,2'}\right)} + \frac{\left(\theta' - \frac{\pi}{4}\right)y_{1,1'} - \left(\theta_{1,1'} - \frac{\pi}{4}\right)\left(y_{1,1'} - y_{2,2'}\right)}{\left(y_{0,2} - y_{2,2'}\right)}, \tag{7}$$

After substitution into Eq. (7) corresponding values from Fig. 2(a), the average stress at the nodal point 0.0 will be the following:

$$\frac{\sigma_{0,0}}{2k} = -1,67 \rightarrow \sigma_{0,0} = -2k \times 1,67, \tag{8}$$

The mean stress components at the central nodal point 0.0 are determined from the following expressions:

$$\sigma_{x_{0,0}} = \sigma_{0,0} + k\sin 2\theta_{0,0} = -2k \times 1,17 \tag{9.a}$$

$$\sigma_{y_{0,0}} = \sigma_{0,0} - k\sin 2\theta_{0,0} = -2k \times 2,17 \tag{9.b}$$

$$\tau_{xy_{0,0}} = -k\cos 2\theta_{0,0} = 0, \tag{9.c}$$

Similarly, the average stress at point 0.1 (lying along the larger diagonal of the metallic material or sample) and its components are determined:

$$\sigma_{0,1} = \sigma_{0,0} - 2k\left(\theta_{0,1} - \pi/4\right) = -2k(1,67 + \pi/18) = -2k \times 1,84 \tag{10.a}$$

$$\sigma_{x_{0,1}} = \sigma_{0,1} + k\sin 2\theta_{0,1} = -2k \times 0,94 \tag{10b}$$

$$\sigma_{y_{0,1}} = \sigma_{0,1} - k\sin 2\theta_{0,1} = -2k \times 2,74 \tag{10.c}$$

$$\tau_{xy_{0,1}} = -k\cos 2\theta_{0,1} = 0,342k, \tag{10.d}$$

The same values of the average stress and its components will be at the nodal point 1.1' (lying along the minor diagonal of the metal material or sample), except that the shear stress will be with a minus sign:

$$\tau_{xy_{1,1'}} = -k\cos 2\theta_{1,1'} = -0,342k. \tag{11}$$

To analyze and calculate the magnitude of shear strains, the concept of true strain ε is introduced, which is a logarithmic or equivalent (cumulative) strain measure. The equivalent strain is calculated using the von Mises and Hencky approaches. The von Mises strain satisfies the properties of both simple and pure shear (Thiel et al., 2018), while the Hencky strain does not satisfy the properties of simple shear. For this reason, the von Mises approach is the most preferred for measuring the equivalent strain in simple shear. Therefore, in the framework of this study, the analysis of shear strains was carried out using the von Mises approach by simulating the rolling of a metal material by the finite element method on the commercial FEM code DEFORM-3D.

4. Results and discussion

The results of the stress analysis indicate that compressive shear stresses act along the small diagonal of the sample, which can lead to chipping and destruction of the material along this diagonal, and tensile shear stresses act along the large diagonal, which intensively displace the metal into the gap between the rolls or into the pass.

The minus values of the average stresses and its components correspond to the same minus values in the average stress distribution pattern obtained by FEM simulation of the metal material rolling in the first diamond pass (the pattern is shown separately in Fig. 3 with a distribution histogram).
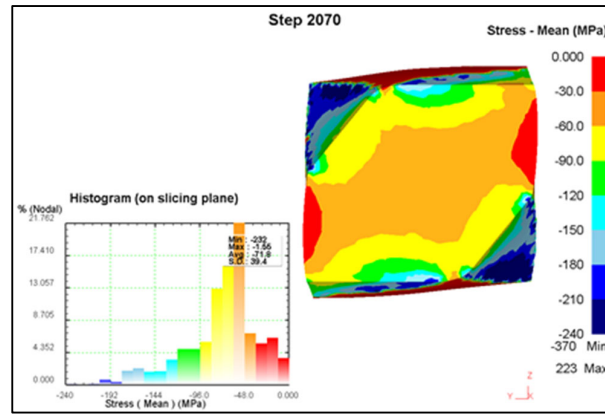
Fig. 3. The picture of the average stress with a histogram of their distribution in the plastic deformation zone, obtained by FEM simulation of the rolling of a metal material in the first diamond pass

The distribution pattern of mean stresses shows the stresses localization along the small and large diagonals. This explains the point reflection or point inversion of the slip lines in Fig. 2, relative to the center point 0.0, which in this case is the inversion point or homothetic center. The point inversion of the slip lines grids relative to the inversion point 0.0 is similar to that of the slip grids rotation of the lines (the grids lying above the x-axis in Fig. 2) by 180°, as shown in Fig. 4.
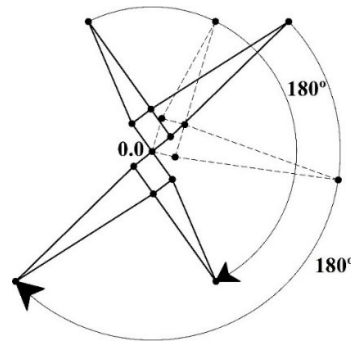

Fig. 4. Point inversion or 180º rotation of slip line grids relative to inversion point or nodal point 0.0.

The von Mises strain obtained by FEM simulation of the metal material rolling in the first diamond pass also demonstrates that under simple shear, there is an X-shaped strain localization along two approximately perpendicular sample diagonals (Fig. 5). Localization or strain nonuniformity is similar to the X-shaped localization observed in the usual upsetting process (Ashkeyev et al., 2023), but with point symmetry rather than line symmetry. Such deformation localization is due to the influence of shear, compression, and friction forces. In the cross-section of a diamond workpiece, deformations are localized along the small diagonal of the diamond workpiece, and minimal deformations are observed along the large diagonal, which is fully consistent with the results of the previous study by the authors (Abishkenov et al., 2022).
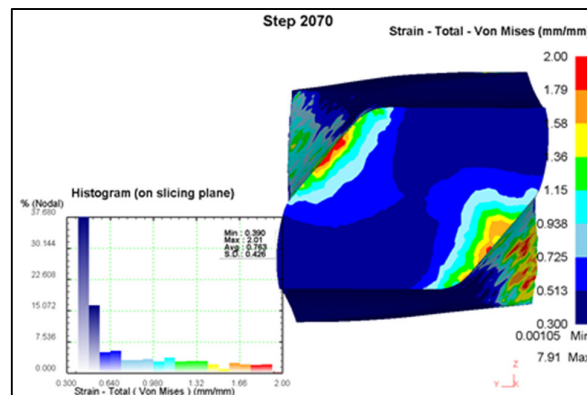

Fig. 5. The von Mises strain with a histogram of their distribution in the plastic deformation zone, obtained by FEM simulation of rolling a metal material in the first diamond pass.

In a material deformed by both compression and shear, an X-shaped zone of localization of the largest deformations will be observed, with the only difference being that with a symmetrical application of external loads (with deformation with compression, that is, without shear); i.e., localization will be linearly symmetrical, whereas shear deformations are pointwise symmetric.

Due to compressive stresses of –0.342k acting along the small diagonal, chipping and destruction of the sample can occur, especially when rolling low-ductile, brittle materials. Under the action of tensile shear stresses of +0.342k, a part of the material, sliding along the contact surface, forms a small local flow towards the larger diagonal. This is how one can explain once again the stress localization phenomenon by point inversion and nonuniform deformation.

5. Conclusions

In general, the results of the stress state analysis show that compressive stresses act at the central nodal point 0.0, preventing the metal destruction along the longitudinal axis X and promoting intensive closure and elimination of all internal defects throughout the entire cross-section of the material. The inhomogeneous deformation under different temperature conditions adversely affects the quality of the material, contributing to the anisotropy of properties: during cold plastic deformation, the material will be nonuniformly hardened, and during hot deformation, recrystallized grains of nonuniform size will be formed. The inhomogeneous deformation during upsetting without shear causes dangerous tensile stresses to form in the central axial zone of the material. Therefore, it would be more expedient to combine compressive deformation with shear, as in the process of shear rolling (Abishkenov et al., 2022).

Since the directions of simple shear in the diamond passes are directed oppositely in the proposed shear rolling process and square passes are located between the diamond passes, the negative effects of deformations are eliminated, which creates prerequisites for using the rolling technology for various metallic materials, including metal-matrix composites.

Acknowledgment

References

Abishkenov, M., Ashkeyev, Z., & Nogaev, K. (2022). Investigation of the shape rolling process implementing intense shear strains in special diamond passes. *Materialia, 26*, 101573.

Afifeh, M., Hosseinipour, S.J., & Jamaati, R. (2019). Nanostructured copper matrix composite with extraordinary strength and high electrical conductivity produced by asymmetric cryorolling. *Materials Science and Engineering: A, 763*, 138146.

Ashkeyev Zh. A., Andreyachshenko VA, & Bukanov Zh. U. (2020). Research of the asymmetric rolling of workpieces. *PNRPU Mechanics Bulletin, 4*, 27–35.

Ashkeyev, Z., Abishkenov, M., & Nogaev, K. (2023). Stress state of workpieces during upsetting with additional shear. *Engineering Solid Mechanics, 11*(1), 41-46.

Ashkeyev, Z., Abishkenov, M., Mashekov, S., & Kawałek, A. (2021). Stress state and power parameters during pulling workpieces through a special die with an inclined working surface. *Engineering Solid Mechanics, 9*(2), 161–176.

Ashkeyev, Z., Abishkenov, M., Mashekov, S., Kawałek, A., & Nogaev, K. (2021). Study of the deformation state during the pulling of the workpiece in a special die. *Metalurgija, 60*(3-4), 335–338.

Bagherpour, E., Pardis, N., Reihanian, M., & Ebrahimi, R. (2019). An overview on severe plastic deformation: research status, techniques classification, microstructure evolution, and applications. *The International Journal of Advanced Manufacturing Technology, 100*, 1647–1694.

Beausir, B., Scharnweber, J., Jaschinski, J., Brokmeier, H.-G., Oertel, C.-G., & Skrotzki, W. (2010). Plastic anisotropy of ultrafine grained aluminum alloys produced by accumulative roll bonding. *Materials Science and Engineering: A, 527*(13-14), 3271–3278.

Beygelzimer, Y., Varyukhin, V., Synkov, S., & Orlov, D. (2009). Useful properties of twist extrusion. *Materials Science and Engineering: A, 503*(1-2), 14–17.

Bridgman, P. W. (1935). Effects of High Shearing Stress Combined with High Hydrostatic Pressure. *Physical Review, 48*(10), 825–847.

Camilo Magalhães, D.C., Cintho, O.M., Rubert, J.B., Sordi, V.L., & Kliauga, A.M. (2020). The role of shear strain during Accumulative Roll-Bonding of multilayered composite sheets: Pattern formation, microstructure and texture evolution. *Materials Science and Engineering: A, 796*, 140055.

Cao, Y., Ni, S., Liao, X., Song, M., & Zhu, Y. (2018). Structural evolutions of metallic materials processed by severe plastic deformation. *Materials Science and Engineering: R: Reports, 133*, 1–59.

Cheng, Y.Q., Chen, Z.H., & Xia, W.J. (2007). Drawability of AZ31 magnesium alloy sheet produced by equal channel angular rolling at room temperature. *Materials Characterization, 58*(7), 617–622.

Cui, Q., & Ohori, K. (2000). Grain refinement of high purity aluminum by asymmetric rolling. *Materials Science and Technology, 16*(10), 1095–1101.

Derakhshan, J.F., Parsa, M.H., & Jafarian, H.R. (2019). Microstructure and mechanical properties variations of pure aluminum subjected to one pass of ECAP-Conform process. *Materials Science and Engineering: A, 747*, 120–129.

Edalati, K., Matsuda, J., Yanagida, A., Akiba, E., & Horita, Z. (2014). Activation of TiFe for hydrogen storage by plastic deformation using groove rolling and high-pressure torsion: Similarities and differences. *International Journal of Hydrogen Energy, 39*(28), 15589–15594.

Huang, J.Y., Zhu, Y.T., Jiang, H., & Lowe, T.C. (2001). Microstructures and dislocation configurations in nanostructured Cu processed by repetitive corrugation and straightening. *Acta Materialia, 49*(9), 1497-1505.

Huang, Y., & Prangnell, P.B. (2007). Continuous frictional angular extrusion and its application in the production of ultrafine-grained sheet metals. *Scripta Materialia, 56*(5), 333-336.

Jamaati, R., & Toroghinejad, M. R. (2014). Effect of stacking fault energy on deformation texture development of nanostructured materials produced by the ARB process. *Materials Science and Engineering: A, 598*, 263–276.

Langdon, T.G. (2010). Processing by severe plastic deformation: historical developments and current impact. *Materials Science Forum, 667–669*, 9–14.

Lee, HH, Yoon, JI, & Kim, HS (2018). Single-roll angular-rolling: A new continuous severe plastic deformation process for metal sheets. *Scripta Materialia, 146*, 204-207.

Lee, J.-C., Seok, H.-K., Han, J.-H., Chung, & Y.-H. (2001). Controlling the textures of the metal strips via the continuous confined strip shearing(C2S2) process. *Materials Research Bulletin, 36*(5-6), 997–1004.

Lee, SH, Saito, Y., Sakai, T., & Utsunomiya, H. (2002). Microstructures and mechanical properties of 6061 aluminum alloy processed by accumulative roll-bonding. *Materials Science and Engineering: A, 325*(1-2), 228–235.

Li, J., Gao, H., Kong, C., Tandon, P., Pesin, A., & Yu, H. (2021). Mechanical properties and thermal stability of gradient structured Zr via cyclic skin-pass cryorolling. *Materials Letters, 302*, 130406.

Mashekov, S., Nurtazaev, E., Mashekova, A., & Abishkenov, M. (2021). Extruding aluminum bars on a new structure radial shear mill. *Metalurgija, 60*(3-4). 427–430.

Mirsepasi, A., Nili-Ahmadabadi, M., Habibi-Parsa, M., Ghasemi-Nanesa, H., & Dizaji, A.F. (2012). Microstructure and mechanical behavior of martensitic steel severely deformed by the novel technique of repetitive corrugation and straightening by rolling. *Materials Science and Engineering: A, 551*, 32–39.

Naizabekov, A.B., & Ashkeev, Z.A. (1995). Analysis of forming and closing of an internal axial defect of a billet. *Steel in Translation, 25*(2), 51–54.

Naizabekov, A.B., & Ashkeev, Zh. A. (1998). Billet state and quality during deformation in special appliance. *Steel in Translation, 28*(8), 52–55.

Naizabekov, A.B., Ashkeev, Zh. A., & Lezhnev, S.N. (1999). Role of shear strains in closing internal defects. *Steel in Translation, 29*(10), 64–66.

Naizabekov, A.B., Bykhin, MB, Nogaev, KA, & Bykhin, BB (2010). Study of the process of realization of high-rate plastic deformation in lengthwise rolling. METAL 2010 - *19th International Conference on Metallurgy and Materials*, 192–202.

Najzabekov, A.B., Nogaev, KA, & Ashkeev, Zh. A. (2004). Deformation of billets with plane block heads with imposing the additional shears of deformation. *Izvestiya Ferrous Metallurgy, 6*, 24–26.

Peng, J., Zhang, Z., Yang, P., Li, Y., Guo, P., Zhou, W., & Wu, Y. (2018). The effect of continuous confined strip shearing deformation on the mechanical properties of AZ31 magnesium alloys. *Materials Science and Engineering: A, 743*, 397–403.

Rahimi Goloujeh, M., & Soltanpour, M. (2021). Simple shear forging as a method for severe plastic deformation. *International Journal of Lightweight Materials and Manufacture, 4*(2), 165–178.

Rees, DWA (2006). *Basic Engineering Plasticity: An Introduction to Engineering and Manufacturing Applications*. Oxford: Butterworth-Heinemann.

Saito, Y., Utsunomiya, H., Suzuki, H., & Sakai, T. (2000). Improvement in the r-value of aluminum strip by a continuous shear deformation process. *Scripta Materialia, 42*(12), 1139-1144.

Saito, Y., Utsunomiya, H., Tsuji, N., & Sakai, T. (1999). Novel ultra-high straining process for bulk materials—development of the accumulative roll-bonding (ARB) process. *Acta Materialia, 47*(2), 579-583.

Song, D., Zhou, T., Tu, J., Shi, L., Song, B., Hu, L., Yang, M., Chen, Q., & Lu, L. (2018). Improved stretch formability of AZ31 sheet via texture control by introducing a continuous bending channel into equal channel angular rolling. *Journal of Materials Processing Technology, 259*, 380–386.

Thiel, C., Voss, J., Martin, RJ, & Neff, P. (2018). Shear, pure and simple. *International Journal of Non-Linear Mechanics, 112*, 57–72.

Utsunomiya, H., Hatsuda, K., Sakai, T., & Saito, Y. (2004). Continuous grain refinement of aluminum strip by conshearing. *Materials Science and Engineering: A, 372*(1-2), 199–206.

Valiev, RZ, Islamgaliev, RK, & Alexandrov, IV (2000). Bulk nanostructured materials from severe plastic deformation. *Progress in Materials Science, 45*(2), 103–189.

Verma, R., Jayaganthan, R., Nath, SK, & Srinivasan, A. (2020). Effect of multiaxial forging followed by hot rolling on non-basal planes and its influence on tensile and fracture toughness behavior of Mg–4Zn–4Gd alloy. *Materials Science and Engineering: A, 774*, 138890.

262

Xu, C., Schroeder, S., Berbon, PB, & Langdon, T. G. (2010). Principles of ECAP–Conform as a continuous process for achieving grain refinement: Application to an aluminum alloy. *Acta Materialia, 58*(4), 1379-1386.

Xu, Q., Li, Y., Ding, H., M, A., Jiang, J., Chen, G., & Chen, Y. (2021). Microstructure and mechanical properties of SiCp/AZ91 composites processed by a combined processing method of equal channel angular pressing and rolling. *Journal of Materials Research and Technology, 15*, 5244–5251.

Yu, H., Wang, L., Chai, L., Li, J., Lu, C., Godbole, A., Wang, H., & Kong, C. (2019). High thermal stability and excellent mechanical properties of ultrafine-grained high-purity copper sheets subjected to asymmetric cryorolling. *Materials Characterization, 153*, 34–45.

Zherebtsov, SV, Dyakonov, GS, Salem, AA, Sokolenko, VI, Salishchev, GA, & Semiatin, SL (2013). Formation of nanostructures in commercial-purity titanium via cryorolling. *Acta Materialia, 61*(4), 1167-1178.

Zhu, XD, Xu, XJ, Zhao, ZH, Chong, K., Cheng, C., & Cheng, XN (2010). The Novel Continuous Large Deformation Technology Integrating Conventional Rolling with Equal-Channel Angular Technology. *Materials Science Forum, 667-669*, 127-132.